#558: Analysis of H2 production with zero carbon emissions from an integrated multi-energy system

Shoaib Ahmed KHAN[1], Jie JI[2*], Wei HE[3**]

[1] Department of Thermal Science and Energy Engineering, University of Science and Technology of China, Hefei, 230026, Anhui, China;
[2] Key Laboratory of Solar Thermal Conversion of Anhui Province, Hefei, 230026, Anhui, China
[3] Department of Building Environment and Equipment, Hefei University of Technology, Hefei 230009, China

Abstract: In this study, a novel system was designed and analyzed experimentally by integrating 8 integrated panels of flat-plate photovoltaic thermal (FP PV/T) producing 1600 W and 2 series connected proton exchange membrane (PEM) electrolyzer to produce green hydrogen, electrical and thermal energy. The numerical model was established for FP PV/T driven PEM electrolyzer and physical model was investigated for key factors to analyze the efficiency and performance of the proposed system. Experimental analysis shows that the temperature and current density play a key role in the production and efficiency of the electrolyzer. However, increasing the FP PV/T temperature also affects electrical efficiency negatively, and the effect of applied current density is larger as compared to inlet temperature. For the membrane thickness of 300 μm, PEM electrolyzer showed the best performance. In simultaneous heat and hydrogen production mode of novel system, the overall solar energy utilization efficiency, hydrogen production efficiency, hydrogen production capacity, and thermal efficiency were 25.52%, 10.01%, 1299.33L, and 15.51% respectively. The system was validated and the relative errors in hydrogen production efficiency, photovoltaic electrical efficiency, electrolyzer efficiency, and hydrogen productionwere 7%, 1.4%, 5.8%, and 5.8%, respectively. The economic analysis shows that the novel system needs additional equipment as compared to conventional solar powered PEM electrolyzer, which increases the initial cost however it proves to be more economical in the longer time span and returns its value in 5 years. The experimental results show that the model can be implemented as a standalone system to fulfill energy needs, or it can be considered as a prototype for energy and hydrogen production on the large scale.

Keywords: Green Hydrogen, Multi-Energy System, Photovoltaic Thermal, Water Electrolysis

1. INTRODUCTION

Background and motivation

The increasing demands of energy, climate change, population growth and rising living standards urge researchers to find new ways of producing clean energy. Hydrogen is considered as the best replacement for fossil fuel in the near future because its only byproduct is water. A research study shows China is the leading country in the hydrogen production technologies due to strong support from government, market trends and technological evolution (Fan et al., 2021). Hosseini SE et al. (2016) found that Hydrogen had better energy efficiency as compared to fossil fuel and it had positive effects on environment (Hosseini and Wahid, 2016). Agyekum EB et al. (2022) investigated the increasing need of hydrogen production methods (Agyekum et al., 2022). Suleman F et al. studied hydrogen, produced from both fossil fuels and renewable sources and found that hydrogen produced by steam methane reforming (SMR) was the most efficient but the most hazardous method to environment (Suleman et al., 2016). Commercially, hydrogen is still produced from fossil fuels. However, Darabadi Zare et al. (2024) proposed the idea to carefully collect carbon dioxide from the gasification process using copper chlorine cycles (Darabadi Zare and Yari, 2024). Acar C et al. (2014) found that producing hydrogen from nuclear energy and water electrolysis under high pressure was a promising solution (Acar and Dincer, 2014). Arsad SR et al. (2024) found the growing trend of hydrogen production from electrolysis and biomass as renewable resources in a patent (Arsad et al., 2024). Younas M et al. (2022) found that generating hydrogen form electrolysis is one of the best renewable energy methods because it gives almost pure hydrogen (Younas et al., 2022).

Literature review

The most common electrolysis methods to produce hydrogen from electrolysis are: Alkaline Electrolysis (AE), Solid Oxide Electrolysis (SOE), Proton Exchange Membrane (PEM) electrolysis and Anion Exchange Membrane (AEM) electrolysis (El-Shafie, 2023). AE was first introduced by Diemann in 1789. It has lower capital cost, but it operates on lower current densities and has higher maintenance cost (Carmo et al., 2013). There is also a great chance of contamination of hydrogen during the production process due to separating diaphragm. SOE technology was first studied by (Dönitz and Erdle, 1985). SOE is used commercially to produce hydrogen on a large scale but there is still enough room to improve the durability and cost. AEM electrolysis uses potassium hydroxide as an electrolyte to produce hydrogen and it is operated at lower temperature and lower current densities as compared to PEM electrolyzer (Li and Baek, 2021). In a study, it was investigated that the comparison of AEM and PEM and found that AEM electrolyzer had higher Faradic efficiency however, PEM needed less energy to operate (Stojić et al., 2008). A comparative study on AEM and PEM and showed that the lye concentration could affect the performance of AEM electrolyzer (Hu et al., 2022). PEM electrolysis was first developed by Thomas Grubb and Leonard Niedrach in 1955 in an experiment performed at General Electric Company (Andújar and Segura, 2009). PEM electrolysis has many advantages over other systems, i.e., it can operate on higher current densities and pressure, it has lower operational cost and lower Ohmic losses and produced hydrogen is 99.9% pure. Slade S et al. (2002) compared different types of membranes for producing hydrogen at large scale and discovered that, PEM electrolyzer required thicker membrane especially when the pressure exceeded 100 bars (Slade et al., 2002).

The idea to harvest both electrical energy and useful thermal energy from solar systems was first presented in 1976 (Wolf, 1976). Another study showed that the hybrid PV/T system used water as working fluid in the collector to reduce the building heating cost for domestic use in longer run (Dubey and Tiwari, 2009). A study shows that water based glazed PV/T collector fulfils the thermal and electrical demands and the glazed PV/T had higher efficiency than unglazed PV/T (Yazdanifard et al., 2016). Water based hybrid PV/T has excellent performance as compared to air-based PV/T (Su et al., 2016). Researchers proposed a hybrid PV/T system to meet the demand of both hot air and water for different seasons and requirement (Wang et al., 2022). They also found that air-based PV/T gave higher thermal efficiency but lower electrical efficiency than water-based PV/T. Water-based flat plate type PV/T increases the electrical efficiency, extracted useful thermal energy and occupies less space as compared to two independent systems for PV and thermal systems (Aste et al., 2014). Another study shows that water-based PV/T by increasing the flow rate of water, electrical efficiency increased while thermal efficiency decreased (Ji et al., 2006). PEM electrolyzer efficiently operates between the temperature range of 50 ℃ and 80 ℃ and requires optimum electrical input to start the electrolysis (Schröder et al., 2004). PV system was used to power up the PEM electrolyzer to produce hydrogen (Lodhi, 1997). MATLAB simulations showed promising results from simulations (Ismail et al., 2019). A theoretical study on feasibility of solar-powered hydrogen system in Algeria found that the system could produce maximum of 29m ^{3} of hydrogen per year (Ghribi et al., 2013). PV system just provides electrical input to the PEM electrolyzer but it also needs hot water. To address this issue, (Salari et al., 2022) carried out numerical study to predict the performance of hydrogen with various PV/T collectors including phase change materials (PCM) and thermoelectric generator (TEG) and found that PV/T performs very well in cost reduction and obtaining hydrogen in more efficient way. Low power solar-powered single PEM electrolyzer proved to be a sustainable method of hydrogen production (Arunachalam and Han, 2024). The system was not directly driven by solar system, PV/T was used to charge a battery and that battery powered up the PEM electrolyzer.

2. INTENT

Contributions and objectives of the proposed system

The literature study shows mostly that previous studies include numerical, or simulation works, however, there is not enough experimental study about solar powered PEM electrolyzers. Previous study also shows that all the numerical studies were conducted on very low power single PV panel driven electrolyzers. Nobody has conducted experiments on a high-power PV/T driven system. The novel system utilizes both electrical and thermal power from solar irradiation by integrating FP PV/T with PEM water electrolyzer. Key contributions and objectives of the system in this paper are.

1. Developing a dynamic mathematical and simulation model for an integrated system which is composed of 1600 W flat-plate PV/T and PEM electrolyzer system.
2. Developing a system which can produce 99.99% pure hydrogen with zero carbon emissions, electricity and hot water.
3. Addressing the cold-start issue of the system and keeping the temperature of electrolyzer in optimal range.
4. Analyzing the system for key factors which affect the efficiency and performance of the system, i.e., solar irradiation, temperature, electrical efficiency, thermal efficiency, current density and membrane-thickness.
5. Performing economic analysis for the proposed system and a conventional solar driven PEM electrolyzer system.
6. Conducting uncertainty analysis and validating the proposed model.

3. METHODS

Electrical power of the FP PV/T system powers up PEM electrolyzer and heat is transferred from PV cells to water for electrochemical reaction and building heating purposes.

3.1. PEM electrolyzer

PEM electrolyzer has compact structure and quick response time with speed of 168-701 milliseconds and requires deionized water to start the electrolysis. FP PV/T was directly coupled with two PEM electrolyzers, each electrolyzer comprised of 5 pairs of series-connected electrodes and membranes. The theoretical maximum hydrogen production rate was 6 L/min, the rated current produced by FP PV/T was 80 A, and the rated power was 1600W. In PEM electrolyzer, membrane electrode assembly (MEA) is the key part of the electrolyzer and it is composed of anode and cathode electrodes, catalytic layers, thin gas diffusion layers (GDL), porous transport layers (PTL) and membrane. The electrodes are coated with a platinum catalyst layer to enhance the electrochemical reaction and electrical conductivity. In thi study, the Nafion membrane was used which only allows only protons to pass through it. Water breakdown reaction is followed as:

Equation 37: Basic water breakdown equation $$H_2O_l \rightarrow H_{2,g} + \frac{1}{2}O_{2,g}$$

Equation 38: HER on cathode side $$2H_2O_l \rightarrow O_{2,g} + 4H^+ + 4e^-$$

Equation 39: OER on anode side $$2H^+_{a\rightarrow c} + 2e^- \rightarrow H_{2,g}$$

Consider temperature from 20 °C to 80 °C and Antoine's equation for vapor pressure. From the Faraday's law, the number of moles of oxygen produced in the corollary of electro-chemical reaction and estimated rate of production are calculated (Corengia and Torres, 2018).

Equation 40: Moles of oxygen required $$O_{a,gen} = \frac{I}{4F}[mol/s]$$

Equation 41: Moles of hydrogen required $$H_2O_a = \frac{I}{2F}[mol/s]$$

In above Equation 40 and Equation 41 calculates number of moles of water are required to split molecules up into its parental atoms. To calculate the total amount of oxygen, amount of oxygen leaving the anode is subtracted from the sum of oxygen obtained and present in the anode (Görgün, 2006). Although FE does not give the quantitative data of the activity of the catalyst but its calculation is critical (Bandal et al., 2018).

Equation 42: Faradic efficiency $$\eta_{FE} = \frac{n_e n_m F}{i_d} \times 100\%$$

Apart from the partial pressure of ions or molecules, there are also other forces which effect the flow of protons across the membrane.

Equation 43: Resistive forces on the Nafion membrane $$H_2O_{mem} = H_2O_{diff} + H_2O_{osf} + H_2O_{hdp}[mol/s]$$

The system is not ideal and there are many factors which cause the voltage drops. The overall cell voltage can be expressed as;

Equation 44: Voltage drops of the electrolyzer $$V = V_{rv} - V_{ac} - V_{oh} - V_{cn}$$

3.2. FP PV/T

FP PV/T generates and provides electrical and thermal energy to PEM electrolyzer system through a combiner box for electrolysis. It consists of a glass cover, photovoltaic cells, heat-absorbing plates, aluminum tubes, and insulation layers. The heat-absorbing plate is combined with the PV through a lamination process. Photovoltaic (PV) cells convert solar energy into electrical energy, while heat absorbers absorb the thermal energy from the photovoltaic cells and keep them cool. BP0.45 plate heat exchanger was used to achieve better thermal performance. The operational range was from 0.6 MPa to 1.6 MPa pressure, the total heat exchange area was 5 m^2, and the maximum flow capacity was 30 m^3/h. In the PV/T the heat was transferred in the form of conduction, convection and radiation (Al-Tabbakh, 2022). The useful heat can be calculated from the glass cover equation.

Equation 45: Glass cover equation

$$\boldsymbol{m_{gl}C_{gl}\frac{dT_{gl}}{dt} = A_{gl}\begin{bmatrix}\alpha_{gl}I(t) + h_{r,gl-sky}(T_{sky} - T_{gl}) + \\ h_{r,abs-gl}(T_{abs} - T_{gl}) + h_{cn,abs-gl}(T_{abs} - T_{gl}) \\ +h_{r,amb-gl}(T_{amb} - T_{gl})\end{bmatrix}}$$

Equation 46: Simplification of the Equation 45

$$\rho_{gl}C_{gl}d_{gl}\frac{dT_{gl}}{dt} = S\alpha_{gl} + h_{r,gl-sky}(T_{sky} - T_{gl}) + \left(h_{r,abs-gl} + h_{cn,abs-gl}\right)\left(T_{abs} - T_{gl}\right) + h_{r,amb-gl}\left(T_{amb} - T_{gl}\right)$$

Power delivered by PV/T is the sum of electrical power and thermal power and so is the efficiency (Hao et al., 2018).

Equation 47: Total efficiency of FP-PV/T system

$$\boldsymbol{\eta = \eta_{elec} + \eta_{thrm}}$$

Equation 48: Electrical efficiency of FP-PV/T

$$\boldsymbol{\eta_{elec} = \frac{I_{max}V_{max}}{A_{pv}S_i}}$$

In order to calculate efficiency for specific interval of time;

Equation 49: Efficiency for the specific interval

$$\boldsymbol{\eta_{elec} = \frac{\sum IV\Delta t}{S_t A_{pv}}}$$

Equation 50: Simplified form of Equation 49

$$\boldsymbol{\eta_{elec} = \eta_{rf}(1 - \beta_{pv}(T_{pv} - T_{rf}))}$$

In above equation η_{rf}, β_{pv}, T_{pv} and T_{rf} represent reference efficiency, temperature coefficient, temperature of PV panel and reference temperature respectively.

Thermal efficiency of the PV/T is calculated from total useful energy received by PV/T, total active area and solar irradiation (Li et al., 2021).

Equation 51: Thermal efficiency of FP-PV/T system

$$\boldsymbol{\eta_{thm} = \frac{Q_{use}}{A_c S_i}}$$

In order to calculate the total useful heat in terms of mass flow rate, the following equation is considered;

Equation 52: Total useful heat from the solar irradiation

$$\boldsymbol{Q_{use} = m_{fl}H_{csp}(T_o - T_i)}$$

Where m_{fl}, H_{csp}, T_o and T_i are mass flow rate, specific heat capacity of water, outlet temperature and inlet temperature respectively (Kujawa et al., 2018). In order to include thermal losses, the equation is modified using Hottel Whillier's equation (Florschuetz, 1979).

Equation 53: Modification of Equation 52 according to Hottel Whiller''s equation $\boldsymbol{Q_{use} = A_c H_{rf}(Q_s - U_{loss}(T_i - T_{amb}))}$

, Q_s , U_{loss} , T_i and T_{amb} are collector area, heat loss coefficient, inlet temperature and atmospheric temperature respectively. H_{rf} represents heat removal efficiency factor which includes all resistances during heat transfer i.e., absorbed heat, useful heat and heart released (Yu et al., 2020).

Equation 54: Total useful heat including the heat-loss

$$\boldsymbol{Q_{use} = Q_{abs} - Q_{loss} - Q_e}$$

Equation 55: Efficiency factor for heat-removal

$$H_{rf} = \frac{1/U_{loss}}{\frac{LW}{N_{htp}}\left[\frac{1}{LU_{loss}\left(\frac{W}{N_{htp}}-L_{htp}\right)F_f+\frac{L_{htp}}{1+r_p-f^{U_{loss}}}}+\sum_{i=1}^{6}R_i\right]}$$

Equation 56: Coefficient of the heal-loss

$$Q_s = (\tau\alpha)_{pv}S_i$$

For accurate calculations, consider primary efficiency η_p,

Equation 57: Including primary efficiency to make model realistic

$$\eta_{pr} = \frac{\eta_{elec}}{\eta_p} + \eta_{thrm}$$

3.3. FP PV/T driven PEM electrolyzer system

Figure ***1*** shows the operation and schematic diagram of the novel FP PV/T driven PEM electrolyzer system for hydrogen production. Purified and deionized water was stored in the 500 L insulated water tank and then circulated through FP PV/T collector and later fed to PEM electrolyzer. When electrochemical reactions starts, oxygen undergoes oxygen evolution reaction (OER), producing oxygen at anode while hydrogen ions (H^+) undergo hydrogen evolution reaction (HER) through proton exchange membrane, producing hydrogen gas at cathode. Electrolysis is an exothermic process and only a small amount of water is consumed so the remaining water turns into steam and is separated by inline separator and the hot water is sent back to water tank through heat exchanger which further increases the water temperature. Thermocouples were installed at the inlet and outlet of the water tank. Two temperature sensors were also installed inside the water tank with an interval of 15 cm to detect temperature changes inside the water tank. The produced hydrogen was stored in the hydrogen cylinders with a maximum pressure of 200 bars. The water continues to circulate producing hydrogen until the reactants are inadequate or there is power loss at the input. Other main components used in the system include LR8402 - 21 data collectors manufactured by HIOKI Co., Ltd, TBQ-2 solar radiation meter with sensitivity of 9.585 μ V/Wm ^{2}, K-type and T-type thermocouples, and MFM-50 mass flow meter with range of 0-3000SCCM.

The efficiency of an electrolytic cell during a certain period of time can be calculated using the following formula:

Equation 58: Efficiency of the novel system

$$\eta_{PEM} = \frac{\int_{H_2} HHV}{W}$$

In the formula: $\eta_{PEM}, W, \int_{H_2}\ and\ HHV$ represent hydrogen production efficiency, power consumption of the electrolyzer, hydrogen production and high heating value of hydrogen respectively.

Equation 59: Production efficiency

$$\eta_{Helec} = \frac{\int_{H_2} HHV}{Q_s}$$

Where Q_s represents the solar irradiation obtained by PV/T.

Equation 60: Solar irradiation from the sun

$$Q_s = A_{PV}\int_0^1 S_i dt N_P N_s$$

In above equation A_{PV}, S_i, N_P and N_s represent total active area of the PV/T, solar irradiation, number of PV modules in parallel and number of PV modules in series respectively.
Efficiency of total thermal energy used by PEM electrolyzer to produce hydrogen is calculated by:

Equation 61: Thermal energy utilization efficiency

$$\eta_{thm} = \frac{\int_{H_2} HHV + m_{fl} H_{csp}(T_o - T_i)}{A_c S_i}$$

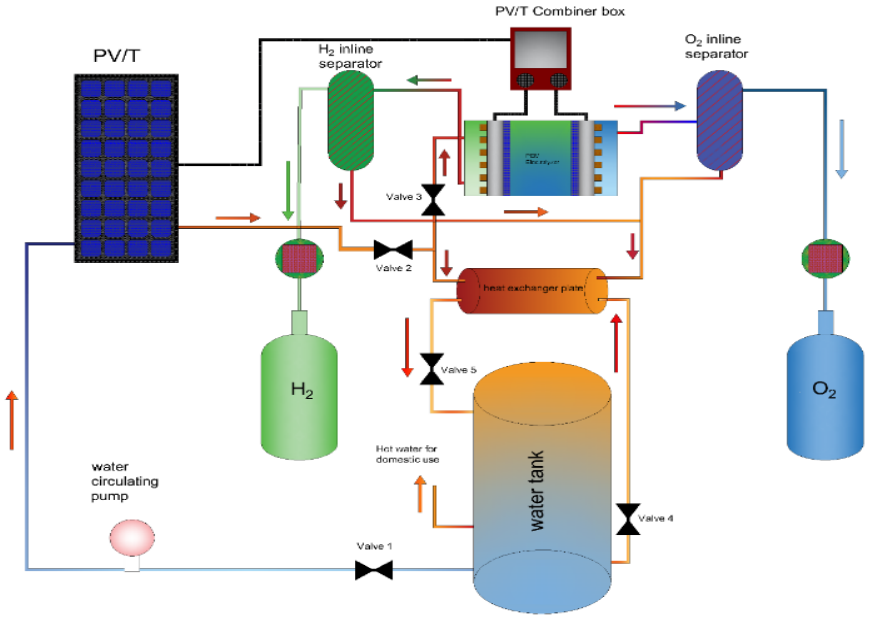

Figure 19: Schematic diagram of the FP PV/T directly coupled with PEM electrolyzer

4. FINDINGS

In FP-PV/T driven PEM electrolyzer the constant flow rate of water was 0.055kg/s, controlled by a water pump. For comparison study the novel model was compared with conventional solar driven PEM electrolyzer system. In case of the conventional solar driven PEM system, a DC power supply was connected to provide constant voltage and maintain the temperature of water in the 23 L HH-601 water tub with constant flow rate of 2 m^3/hr. All the other boundary conditions were the same as explained above.

4.1. Thermal assessment of the novel FP PV/T driven PEM electrolyzer system

Since the novel system can produce both thermal energy and electrical energy at the same time, the thermal analysis was done only for the novel system and it is divided into two parts for better understanding i.e., heating mode and simultaneous heat and hydrogen production mode. In heating mode, the solar irradiation intensity fluctuated between 400 -1100W/m^2 and total received radiation was 160MJ. The ambient temperature varied from 20.19℃ to 30.46℃ resulting in the increase of temperature of 311L water from 19.13℃ to 38.65℃. The system heating capacity was 25.4MJ, and the thermal efficiency of the FP PV/T system was 15.92%, which was much lower than that of a normal PV/T system. The main reason for this is use of bare Aluminum tubes in collector instead of insulated copper tubes. The total radiation received by the FP PV/T during the experiment was 165.9 MJ. The temperature of the remaining 298kg water in the water tank increased from 19.98℃ to 40.55℃. The system heating capacity was 25.74 MJ, and the thermal efficiency was 15.51%. Thermal efficiency in the simultaneous hydrogen and heat production was lower than heating mode because water was gradually consumed in the water tank during the simultaneous hydrogen and heating cycle, which led to direct heat loss to atmosphere. This circulation of water also led to lowering the water quality which also lowered the thermal efficiency of water.

4.2. Effect of electrical efficiency on hydrogen production efficiency on FP-PV/T and conventional PV driven PEM electrolyzer

The hourly FP-PV/T electrical efficiency fluctuated between 11.88% and 13.12%, while the hourly hydrogen production efficiency of the system fluctuated between 8.71% and 10.96%. The pattern of hydrogen production efficiency of the system was roughly synchronous with the PV/T electrical efficiency. The FP PV/T electrical efficiency and hydrogen production efficiency showed bimodal behavior. Increase in solar irradiation increased system performance, but when the temperature of the PV panels increased, the electrical efficiency decreased which led to a decrease in the overall system performance. In the afternoon, temperature of the PV panels gradually decreased and the system performance improved, resulting in a second peak of efficiency. Conventional PV efficiency and hydrogen production efficiency fluctuated between 11.7 % to 13.99% and 9.11 % to 11.75 % respectively. Increasing solar irradiation increases the electrolyzer and PV efficiency, and hence increases hydrogen production. However, increasing the water temperature can effectively improve the efficiency of PEM electrolyzer.

4.3. Effect of temperature on operating point of PEM electrolyzer

The PV cells temperature increased form 25 °C to 75 °C while electrolyzer-temperature was constant at 30 °C, the operating point of the system deviates from the maximum power point tracking (MPPT) point of the system. This phenomenon occurs because when PV temperature increases, electrical efficiency and hydrogen production decrease. 错误!未找到引用源。

(b) shows the increase in temperature of both FP PV/T and PEM electrolyzer from 25°C to 75°C. The operating point of the system again deviated from the MPPT point. Increase in the electrolyzer temperature should improve the operating point, however, the effect on electrical input is big, and electrical efficiency has decreased due to high FP PV/T temperature

4.4. Effect of ambient temperature on the internal temperature of the electrolyzer driven by FP-PV/T systems

In case of the novel FP-PV/T system, the left electrolyzer was placed in a sun, and the right electrolytic cell was placed in shadow, the initial temperature of the left side electrolyzer was 4.57℃ higher. Increase in the solar irradiation increased the current which increased the rate of electrochemical reaction and that increased the internal temperature of the electrolyzer. The temperature of both electrolyzers became constant after a while because both electrolyzers were receiving the same amount of electrical energy.

4.5. Effect of solar irradiation on power delivered by FP PV/T and conventional PV systems

In case of simultaneous heat and hydrogen production, the system performance mainly depended on solar irradiation and temperature of the FP PV/T. During the experiment, the maximum irradiation intensity was 1016.06W/m ^{2} and current delivered by PV/T was 55.93A. This was not the maximum current produced because the temperature affected electrical performance of PV negatively. The voltage of electrolyzer varied from 17.04V to 18.06V, which was almost constant on both sides of the electrolyzer although overall power had fluctuations. The experiment lasted for 7 hours, and the fluctuation range of PV/T electrical efficiency was from 11.57% to 14.21%. In Figure 2 (a), the first peak in electrical efficiency was around 10 am because initially the temperature of PV/T was low but later the solar irradiation increased the water-temperature which increased PV/T-temperature, and this gradually decreased electrical efficiency. The second peak was around 2:30 pm, this was due to a decrease in the PV/T temperature. The circulation of water caused cooling effects, however the solar irradiation decreased gradually. In the case of conventional PV system, apart from solar irradiation, the inlet water temperature also varied, and the output power of the system was highly correlated with the irradiation intensity and inlet water temperature as shown in Figure 2 (b). From three days data, maximum current delivered by PV was 58.335A, 53.115A and 53.98A, maximum output power was 1074.77W, 947.067W, and 954.3934W, solar irradiation was 1047.157W/m^2, 955.55W/m^2 and 970.9963W/m^2 and the constant inlet water temperature of 30℃, 40℃ and 50℃ respectively. This also shows that the system performs better at lower input water temperature, however when the temperature of the PV increases, the overall electrical efficiency decreases abruptly. As compared to conventional solar powered systems, there was no big difference in the electrical efficiency of PV/T. The main reason is that the FP PV/T modules usedin the experiment were covered with glass cover that reflected sunlight and resulted in decline in the efficiency.

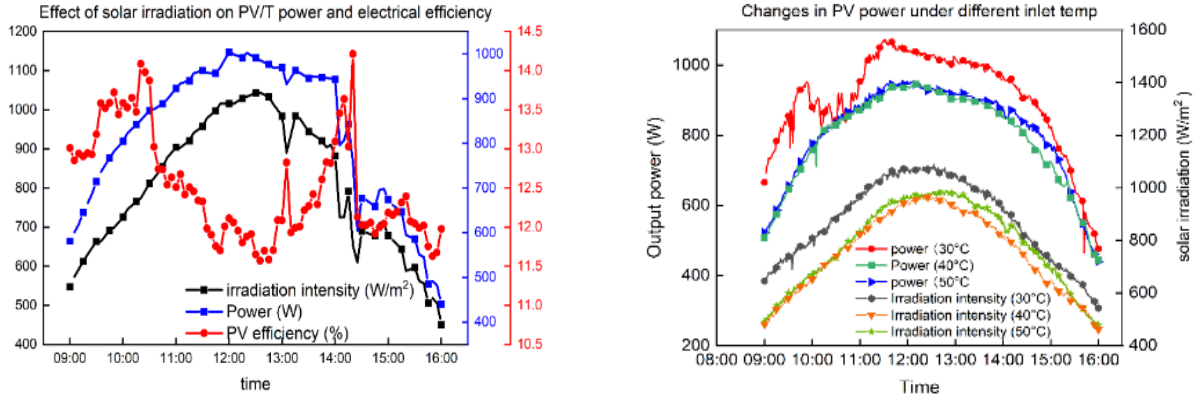

(a) Effect of solar irradiation on FP PV/T power

(b) Effect of solar irradiation on PV power

Figure 20: Effect of solar irradiation on electrical power of solar system

4.6. Effect of solar irradiation on rate and total amount of hydrogen produced by FP-PV/T driven and conventional PV driven PEM electrolyzer system

Figure 3 (a) shows the direct relationship between hydrogen production rate and irradiation intensity and the graph is almost synchronous. The maximum hydrogen production rate on that day was 3627ml/min. Figure 3 (b) shows the hourly average hydrogen production rate and total hydrogen produced which was 3093.65ml/min and 1299.33L respectively. Thisis because when the solar irradiation increases, the electrical power produced by FP PV/T increases, and that power is directly applied to PEM electrolyzer which results in the increase in the hydrogen production. For the conventional PV system, Figure 3 (c) shows that the highest hydrogen production rates for three different days were 4008ml/min, 3664ml/min, and 3836ml/min for 30℃, 40℃, and 50℃ inlet water temperature respectively. It also shows that increasing the irradiation intensity results in increasing the overall hydrogen production. The results also show that the hydrogen production rate and the amount of overall hydrogen produced are affected directly by the inlet water temperature. Total hydrogen produced during the three days of the experiment was 1397.64 L, 1297.27 L, and 1381.03 L respectively. The produced hydrogen was stored in hydrogen cylinder with prescribed maximum pressure of 200 bars.

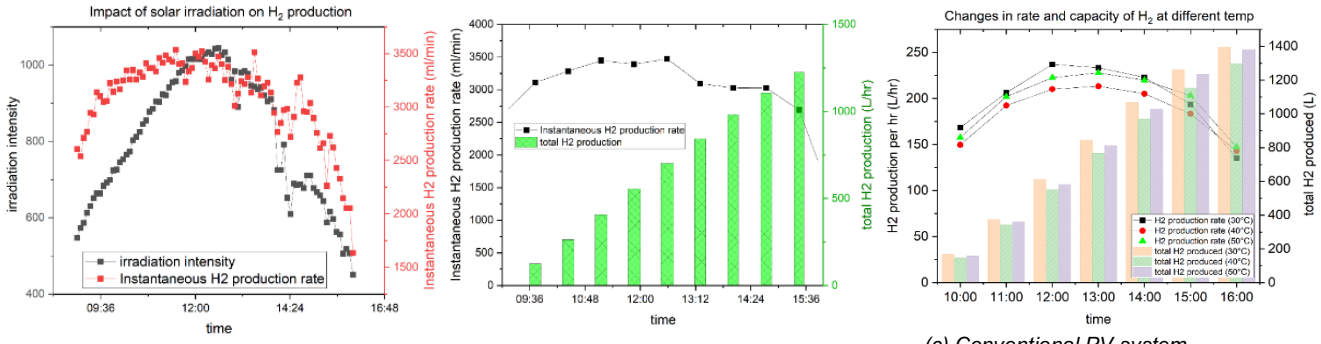

(a) FP-PVT system (b) FP-PVT system *(c) Conventional PV system*

Figure 21: Effect of solar irradiation on instantaneous and total hydrogen production on FP PV/T driven PEM electrolyzer system

4.7. Effect of membrane thickness on the operating point of the PEM electrolyzer

When membrane-thickness was increased from 100 µm to 300 µm, the operating point gradually approached the MPPT point which made the system more efficient overall. When membrane thickness was increased to 500 µm the operating point of the electrolyzer deviated from the MPPT point. Thicker membranes are suitable for electrolyzers working under higher operating pressure.

4.8. Validation of HP PV/T driven PEM electrolyzer system for H_2 production

Figure 4 (a) shows the comparison of both simulation results and experimental results for performance prediction of PEM electrolyzer. The relative error between simulated data and experimental data was 1.36% which shows a good uniformity of both results. In the graph, voltage drops first increase due to ohmic over-potential however it becomes uniform as the current density increases. Increase in current density also increases hydrogen production. It was found that 156MJ cumulative daily solar radiation was received which produced 21.47MJ of total power. System hydrogen production efficiency, electrical efficiency, electrolyzer efficiency and total hydrogen produced were 11.24%, 13.74%, 83.76%, 1374L respectively. The difference between simulation and experiment were 0.62%, 0.9%, 1.17% and 76.73L respectively. The relative errors from the experimental results were 7%, 1.4%, 5.8%, and 5.8%, respectively. The consistency of the results show that the model can be used to predict and improve the performance of PV/T directly coupled PEM electrolyzer for hydrogen production. The solar irradiation was varying according to time, Figure 4 (b) and Figure 4 (c) the temperature of FP PV/T and the PEM electrolyzer increased. By solving the transient model, the voltage and power values were obtained from simulation which were compared with the experimental values. The maximum relative error between simulation results and experimental result was 3.17 % which shows a good agreement of both results and verifies the model to be consistent and reliable.

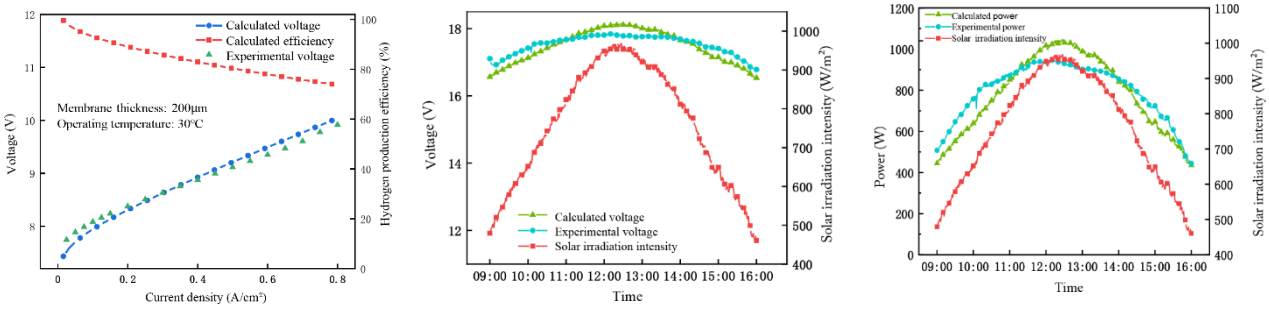

(a) Performance validation (b) Comparison in terms of voltage (c) Comparison in terms of overall power

Figure 22: Validation of power, voltage and performance of FP PV/T driven PEM electrolyzer

5. CONCLUSION

This article presents a dynamic mathematical model and experimental verification of the novel flat-plate PV/T (FP PV/T) technology integrated directly with PEM water electrolyzer for multi=energy and green hydrogen production. In this experimental work, solar energy is the primary source of energy, however, FP PV/T converts that into secondary form of energy i.e., electrical and thermal energy. This electrical energy directly runs the PEM electrolyzer and thermal energy is provided in the form of hot water. The key achievements from the results of this study are as follows.

1. Circulation of water in FP PV/T decreases temperature of PV cells and improves electrical efficiency and hydrogen production.
2. Increasing membrane thickness beyond 300 µm deviates the system performance from MPPT point.
3. Increase in the current density increases the hydrogen production hut it also increases the internal temperature of the electrolyzer and it may damage the membrane if exposed for long time.
4. Conventional solar driven PEM electrolyzer eliminates the need for batteries, DC/DC converters, and other equipment which significantly reduce the operation and maintenance cost. However, this system needs additional

power to get the specific inlet water-temperature.

5 From economic analysis, FP PV/T driven PEM electrolyzer returns the money invested successfully in 5 years. However, the conventional PV driven system needs few more years to return the money invested due to cost of additional power.

For FP PV/T driven PEM electrolyzer system, the solar energy utilization efficiency, hydrogen production efficiency, thermal efficiency and thermal capacity were 25.52%, 10.01%, 15.51% and 25.74MJ respectively. The temperature of 298kg water in the water storage tank increased from 19.98 ℃ to 40.55 ℃ and 1299.33L of hydrogen was produced during 7 hours of experiment. For the novel FP PV/T system, hydrogen production efficiency, electrical efficiency, electrolyzer efficiency and total hydrogen produced were 11.24%, 13.74%, 83.76%, 1374L respectively, the differences between simulation and experiment were 0.62%, 0.9%, 1.17%, and 76.73L,

6. REFERENCES

ACAR, C. & DINCER, I. 2014. Comparative assessment of hydrogen production methods from renewable and non-renewable sources. International Journal of Hydrogen Energy, 39**,** 1-12.

AGYEKUM, E. B., NUTAKOR, C., AGWA, A. M. & KAMEL, S. 2022. A Critical Review of Renewable Hydrogen Production Methods: Factors Affecting Their Scale-Up and Its Role in Future Energy Generation. Membranes [Online], 12.

AL-TABBAKH, A. A. 2022. Numerical transient modeling of a flat plate solar collector. Results in Engineering, 15**,** 100580.

ANDÚJAR, J. M. & SEGURA, F. 2009. Fuel cells: History and updating. A walk along two centuries. Renewable and Sustainable Energy Reviews, 13**,** 2309-2322.

ARSAD, S. R., KER, P. J., HANNAN, M. A., TANG, S. G. H., R S, N., CHAU, C. F. & MAHLIA, T. M. I. 2024. Patent landscape review of hydrogen production methods: Assessing technological updates and innovations. International Journal of Hydrogen Energy, 50**,** 447-472.

ARUNACHALAM, M. & HAN, D. S. 2024. Efficient solar-powered PEM electrolysis for sustainable hydrogen production: an integrated approach. Emergent Materials.

ASTE, N., DEL PERO, C. & LEONFORTE, F. 2014. Water flat plate PV–thermal collectors: A review. Solar Energy, 102**,** 98-115.

BANDAL, H., REDDY, K. K., CHAUGULE, A. & KIM, H. 2018. Iron-based heterogeneous catalysts for oxygen evolution reaction; change in perspective from activity promoter to active catalyst. Journal of Power Sources, 395**,** 106-127.

CARMO, M., FRITZ, D. L., MERGEL, J. & STOLTEN, D. 2013. A comprehensive review on PEM water electrolysis. International Journal of Hydrogen Energy, 38**,** 4901-4934.

CORENGIA, M. & TORRES, A. I. 2018. Two-phase Dynamic Model for PEM Electrolyzer. In: EDEN, M. R., IERAPETRITOU, M. G. & TOWLER, G. P. (eds.) Computer Aided Chemical Engineering. Elsevier.

DARABADI ZARE, A. A. & YARI, M. 2024. Techno economic analysis of efficient and environmentally friendly methods for hydrogen, power, and heat production using chemical looping combustion integrating plastic waste gasification and thermochemical copper chlorine cycles. Energy, 289**,** 129941.

DÖNITZ, W. & ERDLE, E. 1985. High-temperature electrolysis of water vapor—status of development and perspectives for application. International Journal of Hydrogen Energy, 10**,** 291-295.

DUBEY, S. & TIWARI, G. N. 2009. Analysis of PV/T flat plate water collectors connected in series. Solar Energy, 83**,** 1485-1498.

EL-SHAFIE, M. 2023. Hydrogen production by water electrolysis technologies: A review. Results in Engineering, 20**,** 101426.

FAN, L., TU, Z. & CHAN, S. H. 2021. Recent development of hydrogen and fuel cell technologies: A review. Energy Reports, 7**,** 8421-8446.

FLORSCHUETZ, L. W. 1979. Extension of the Hottel-Whillier model to the analysis of combined photovoltaic/thermal flat plate collectors. Solar Energy, 22**,** 361-366.

GHRIBI, D., KHELIFA, A., DIAF, S. & BELHAMEL, M. 2013. Study of hydrogen production system by using PV solar energy and PEM electrolyser in Algeria. International Journal of Hydrogen Energy, 38**,** 8480-8490.

GÖRGÜN, H. 2006. Dynamic modelling of a proton exchange membrane (PEM) electrolyzer. International Journal of Hydrogen Energy, 31, 29-38.

HAO, W., LU, Y., LAI, Y., YU, H. & LYU, M. 2018. Research on operation strategy and performance prediction of flat plate solar collector with dual-function for drying agricultural products. Renewable Energy, 127, 685-696.

HOSSEINI, S. E. & WAHID, M. A. 2016. Hydrogen production from renewable and sustainable energy resources: Promising green energy carrier for clean development. Renewable and Sustainable Energy Reviews, 57, 850-866.

HU, K., FANG, J., AI, X., HUANG, D., ZHONG, Z., YANG, X. & WANG, L. 2022. Comparative study of alkaline water electrolysis, proton exchange membrane water electrolysis and solid oxide electrolysis through multiphysics modeling. Applied Energy, 312, 118788.

ISMAIL, T. M., RAMZY, K., ELNAGHI, B. E., ABELWHAB, M. N. & EL-SALAM, M. A. 2019. Using MATLAB to model and simulate a photovoltaic system to produce hydrogen. Energy Conversion and Management, 185, 101-129.

JI, J., HAN, J., CHOW, T.-T., YI, H., LU, J., HE, W. & SUN, W. 2006. Effect of fluid flow and packing factor on energy performance of a wall-mounted hybrid photovoltaic/water-heating collector system. Energy and Buildings, 38, 1380-1387.

KUJAWA, T., WASIK, M., BUGAJ, M. A., WIŚNIEWSKI, T. S., KLEIN, M., CHAJA, P., BYKUĆ, S., STACHEL, A. A. & ZAPAŁOWICZ, Z. 2018. Mathematical model of flat plate solar thermal collector and its validation. E3S Web ofConferences, 70, 01019.

LI, C. & BAEK, J.-B. 2021. The promise of hydrogen production from alkaline anion exchange membrane electrolyzers. Nano Energy, 87, 106162.

LI, Z., JI, J., YUAN, W., ZHAO, B., ZHOU, F., MUIN UDDIN, M., REN, X., YU, B. & SONG, Z. 2021. Experimental & numerical investigation and optimization on a novel flat-plate PV/T system using CdfTe thin-film solar modules of sandwich structure. Solar Energy, 223, 261-277.

LODHI, M. A. K. 1997. Photovoltaics and hydrogen: Future energy options. Energy Conversion and Management, 38, 1881-1893.

SALARI, A., HAKKAKI-FARD, A. & JALALIDIL, A. 2022. Hydrogen production performance of a photovoltaic thermal system coupled with a proton exchange membrane electrolysis cell. International Journal of Hydrogen Energy, 47, 4472-4488.

SCHRÖDER, V., EMONTS, B., JANßEN, H. & SCHULZE, H. P. 2004. Explosion limits of hydrogen/oxygen mixtures at initial pressures up to 200 bar. Chemical Engineering and Technology, 27, 847-851.

SLADE, S., CAMPBELL, S. A., RALPH, T. R. & WALSH, F. C. 2002. Ionic conductivity of an extruded Nafion 1100 EW series of membranes. Journal of the Electrochemical Society, 149, A1556-A1564.

STOJIĆ, D. L., GROZDIĆ, T. D., UMIĆEVIĆ, B. & MAKSIĆ, A. D. 2008. A comparison of alkaline and proton exchange membrane electrolyzers. Russian Journal of Physical Chemistry A, Focus on Chemistry, 82, 1958-1960.

SU, D., JIA, Y., HUANG, X., ALVA, G., TANG, Y. & FANG, G. 2016. Dynamic performance analysis of photovoltaic–thermal solar collector with dual channels for different fluids. Energy Conversion and Management, 120, 13-24.

SULEMAN, F., DINCER, I. & AGELIN-CHAAB, M. 2016. Comparative impact assessment study of various hydrogen production methods in terms of emissions. International Journal of Hydrogen Energy, 41, 8364-8375.

WANG, C., JI, J., ZHANG, C., KE, W., TANG, Y. & TIAN, X. 2022. Experimental and numerical investigation of a multi-functional photovoltaic/thermal wall: A practical application in the civil building. Energy, 241, 122896.

WOLF, M. 1976. Performance analyses of combined heating and photovoltaic power systems for residences. Energy Conversion, 16, 79-90.

YAZDANIFARD, F., EBRAHIMNIA-BAJESTAN, E. & AMERI, M. 2016. Investigating the performance of a water-based photovoltaic/thermal (PV/T) collector in laminar and turbulent flow regime. Renewable Energy, 99, 295-306.

YOUNAS, M., SHAFIQUE, S., HAFEEZ, A., JAVED, F. & REHMAN, F. 2022. An Overview of Hydrogen Production: Current Status, Potential, and Challenges. Fuel, 316, 123317.

YU, Q., HU, M., LI, J., WANG, Y. & PEI, G. 2020. Development of a 2D temperature-irradiance coupling model for performance characterizations of the flat-plate photovoltaic/thermal (PV/T) collector. Renewable Energy, 153, 404-419.